Available on CMS information server

CMS NOTE 2006/072

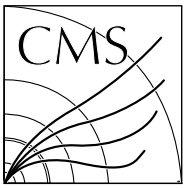

The Compact Muon Solenoid Experiment

CMS Note

Mailing address: CMS CERN, CH-1211 GENEVA 23, Switzerland

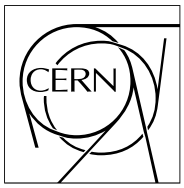

16 May 2006

Results of the First Integration Test of the CMS Drift Tubes Muon Trigger

C. Deldicque, J. Erö

Institute for High Energy Physics of the Austrian Academy of Sciences, Nikolsdorfergasse 18, A-1050, Wien, Austria

M. Bontenackels, T. Hebbeker, K. Hoepfner, H. Reithler, P. Ruetten, M. Sowa

III. Physikalisches Institut der RWTH Aachen, D-52056 Aachen, Germany

C. Battilana, A. Benvenuti, F.R. Cavallo, G.M. Dallavalle, P. Giacomelli, M. Giunta, L. Guiducci, S. Marcellini, A. Montanari, F.L. Navarria, F. Odorici, A. Perrotta, T. Rovelli, G. Torromeo, R. Travaglini

INFN and Dipartimento di Fisica dell'Universita', Viale Berti Pichat 6/2, I-40127 Bologna, Italy

G. Maron, N. Toniolo

INFN, Laboratori Nazionali di Legnaro, Viale dell'Universita' 2, I-35020 Legnaro(PD), Italy

M. Bellato, L. Castellani, P. Checchia, E. Conti, F. Gasparini, F. Gonella, S. Lacaprara, A.T. Meneguzzo, A. Parenti, M. Passaseo, P. Ronchese, E. Torassa, S. Vanini, S. Ventura, M. Zanetti, P. Zotto

INFN and Dipartimento di Fisica dell'Universita', Via Marzolo 8, I-35131 Padova, Italy

N. Amapane, G. Cerminara, V. Monaco, A. Staiano

INFN and Dipartimento di Fisica dell'Universita', Via Giuria 1, I-10125 Torino, Italy

M. Aldaya, B. de la Cruz, C. Fernández, M.C. Fouz, I. Josa, J. Puerta, C. Villanueva

CIEMAT - Division de Fisicas de Particulas, Avenida Complutense 22, E-28040, Madrid, Spain

J. Fernández de Trocóniz, I. Jiménez

Universidad Autonoma de Madrid, Ctra. de Colmenar km 15, E-28049 Madrid, Spain

Abstract

Two drift tube stations of the CMS barrel muon system were exposed, in October 2004, to a 40 MHz bunched muon beam at the CERN SpS. The performance of the level-1 local trigger was tested at different energies and inclination angles of the incident muon beam. Data with and without an iron absorber between the two stations were also collected, to simulate the electromagnetic shower development in CMS. In addition, special data-taking runs were dedicated to test the level-1 Track

Finder trigger for the first time. The present note describes the results of the these measurements, focusing the attention on the efficiency and the noise rate of the trigger systems.

1 Introduction

The task of the muon trigger of the CMS experiment at LHC [1], [2], [3] is to provide muon identification and to measure the particle transverse momentum, in order to allow online rate reduction. In addition the system has to assign to each muon candidate the corresponding bunch crossing (BX) already at the hardware level, called level-1 trigger. In the barrel region of the CMS detector, the muon trigger is delivered independently by two subsystems: the resistive plate chambers (RPC) and the drift tubes (DT). Whereas the RPC detector has an excellent time resolution from single hits, which corresponds to a very precise and unambiguos BX determination, accompanied by less precise momentum and position resolution, the DT system can perform a precise momentum measurement associated with a good BX determination based on a fast track reconstruction.

In each muon station the DT local trigger in the $r-\phi$ view, which is the bending plane, provides up to two track segments (trigger primitives) for each BX. The DT track finder (DTTF) system constructs a muon track candidate by performing a matching between the segments delivered by the local trigger in the DT muon stations crossed by the particle. A BX and a transverse momentum value $\mathrm{p_t}$ are assigned to the muon trigger candidate.

In order to test and validate the performance of the barrel muon chamber readout and trigger electronics, a bunched beam is needed, with a time structure similar to the one at the LHC, where proton collisions occur every 25 ns, corresponding to a frequency of 40 MHz. The first complete test of the DT local trigger electronics and of the performance of the corresponding local trigger was made in May 2003 at the CERN SpS using an LHC-like muon beam to which a single muon station was exposed. The results of the measurements performed in this test are described in [4].

In October 2004 an experimental set-up consisting of two muon stations, both equipped with the DT trigger and read-out electronics, was exposed to a 40 MHz muon beam having the same characteristics of the previous test. Data were taken at several incident track inclination angles and impact points, as well as different muon beam momenta, with and without an iron absorber placed between the two muon stations, to reproduce the effect of the material in CMS. This allowed to study the impact of the electromagnetic showers on the trigger performance. In addition, the output of the local trigger of the two muon stations was sent as input to the ϕ DTTF, and the whole DT level-1 trigger chain was then tested for the first time. No magnetic field was available for the measurements. In order to simulate the bending of the muon tracks in the CMS magnetic field, data were taken shifting and tilting one station with respect to the other. This note reports the results of these measurements.

2 The Drift Tubes Local Trigger

The CMS muon barrel drift chambers were already described extensively elsewhere [5]. They are composed of three groups of drift tubes called superlayers (SLs). Each SL is built of four layers of drift tubes, staggered by half a tube width. Two SLs measure muons in the transverse bending plane ($\mathrm{r}-\phi$) of CMS (hereafter ϕ view) and one SL detects them in the longitudinal nonbending ($\mathrm{r}-\theta$) plane (hereafter θ view). The two ϕ SLs are called "inner" or "outer" to identify their position with respect to the center of CMS in the muon station where they are located. A honeycomb panel to give stiffness to the chamber, and a θ SL, separate the two ϕ SLs and provide a lever arm for a better track fitting angular resolution. The CMS muon barrel is assembled in such a way that muons tracks produced in LHC interactions can cross up to four muon stations, placed at different distances from the interaction point. The stations are labeled MB1, MB2, MB3 and MB4, starting from the center of CMS. Each chamber is instrumented with read-out electronics, as well as with bunch and track identifiers (BTIs), track correlators (TRACOs) and a trigger server (TS), which are the basic elements of the DT local trigger chain. The block scheme of the DT electronics mounted on each muon station is shown in figure 1. Details can be found in [4] and references therein.

The logical steps of the DT local trigger are summarised in the following. The local triggers are made out of segments provided by the BTIs in the inner and outer ϕ SLs separately. A BX is also assigned to every segment. The BTI assigns a quality tag to the segment, which is High (H) or Low (L) if in the SL an alignment of four hits, or only three out of four hits is found, respectively. A correlation of the inner and outer segments can be found by the TRACOs, with quality HH, HL, or LL, where H and L is the quality of the matched segments. If the correlation fails, or if one of the two BTIs segments is simply missing, the trigger candidate found by the TRACO will be from one SL only, with quality Ho, Hi, Lo or Li, where "o" and "i" stand for "outer" and "inner", respectively. A local trigger segment is also characterized by the "radial angle" ϕ, and the "incident angle" ϕ_{b}, which are sketched in figure 2. On average there are about 20 TRACOs in each chamber, being as much as 24 for the largest muon station. Each TRACO can deliver up to two track candidates to the TS, related to a physical BX. In the case of the test-beam, a physical BX is a single beam shot. Each TRACO labels its two candidates as "first" and "second"

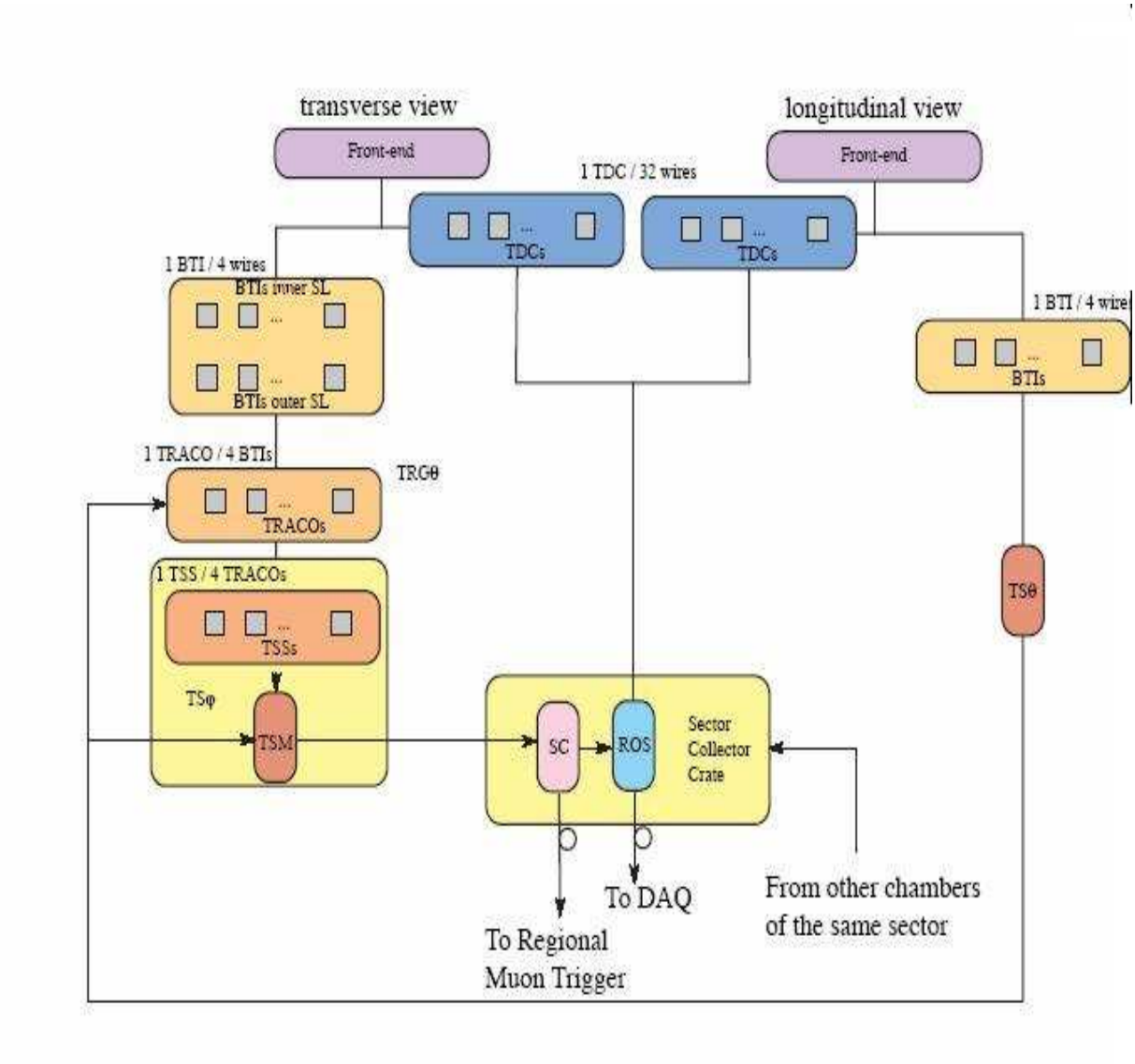

Figure 1: Overview of the main building blocks of a barrel muon station electronics. Transverse and longitudinal view labels correspond to ϕ and θ view respectively.

track, using a programmable priority encoding. The two tracks are multiplexed on the same bus, and therefore the "second track" will be transferred one BX later if there is no new trigger in this next BX.

The TS has to select up to two track segments for each BX, out of at most 40 segments delivered by all the TRACOs in each station [1)]. The two segments selected by the TS should represent, from the physics point of view, the two highest transverse momentum tracks. In practice the sorting algorithm is based on both the quality of the track segments and their bending angle. Several ghost suppression mechanisms are applied by the local trigger, to get rid of the segment copies which can be generated by the system when a single track traverses a muon chamber, due to functional redundancy introduced in BTIs and TRACOs for system robustness. Since the chamber trigger electronics delivers as output at most two muon candidates, ghost track rejection will be very important for reliably selecting di-muon events in LHC pp collisions, if the two muons are very close in space.

A relevant feature of the θ trigger is to validate uncorrelated low quality segments delivered by the ϕ trigger. Such types of segments are in fact delivered by the local trigger of a station to the regional trigger only if a θ trigger segment is also found in the same station at the same BX.

[1)] In normal cases most of such segments will be null tracks.

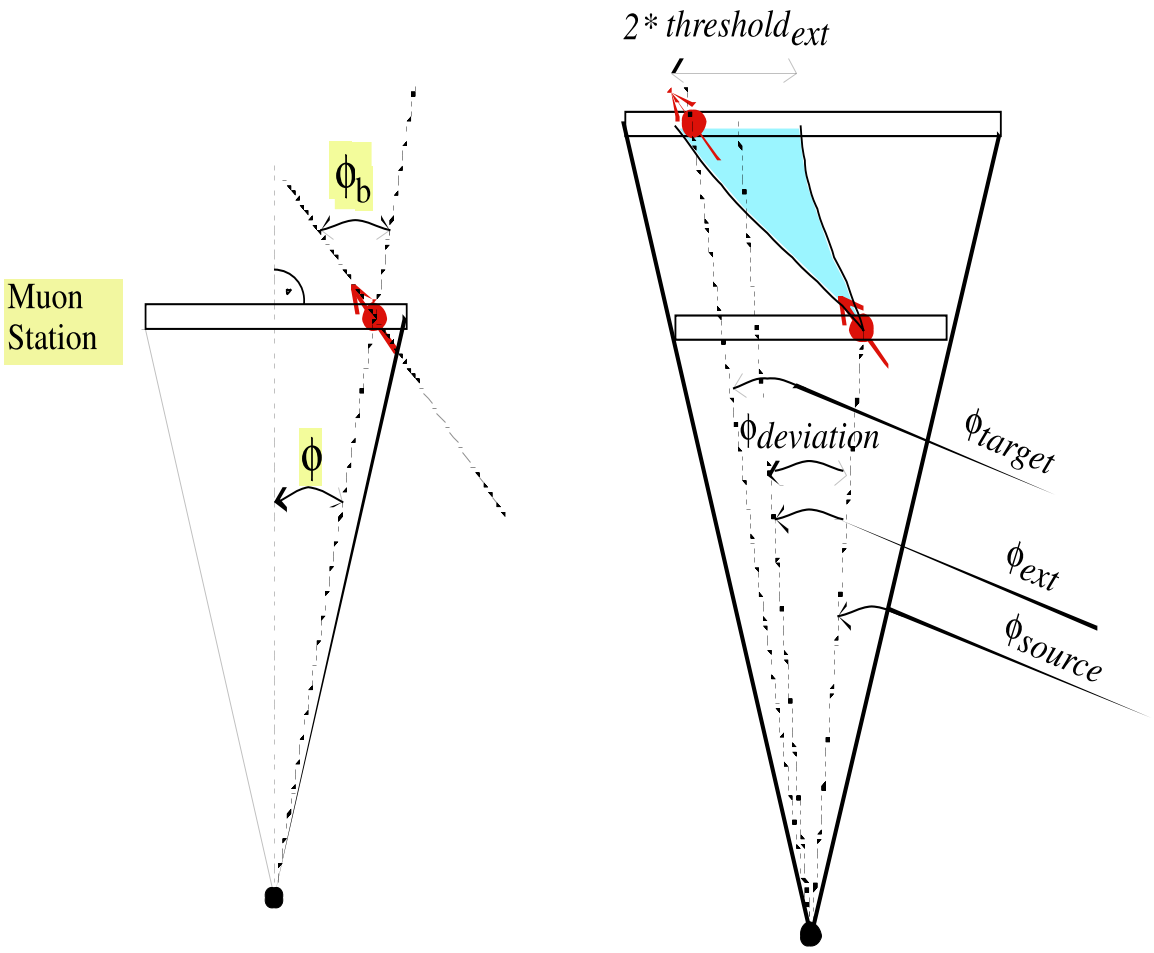

Figure 2: A sketch of the quantities ϕ and $\phi_{\rm b}$ which are delivered by the DT local trigger to the DTTF in each muon station, to construct a track candidate, are shown in the leftmost figure. The angle ϕ, also called "radial angle", defines the displacement of the trigger segment with respect to the center of the muon station. The angle $\phi_{\rm b}$, also called "incident angle", is the angle of the trigger segment with respect to the direction of a track with infinite transverse momentum, crossing the muon station in that position. The rightmost figure shows in a schematic way how DT local trigger segments from a station are extrapolated to another station by the ϕ DTTF.

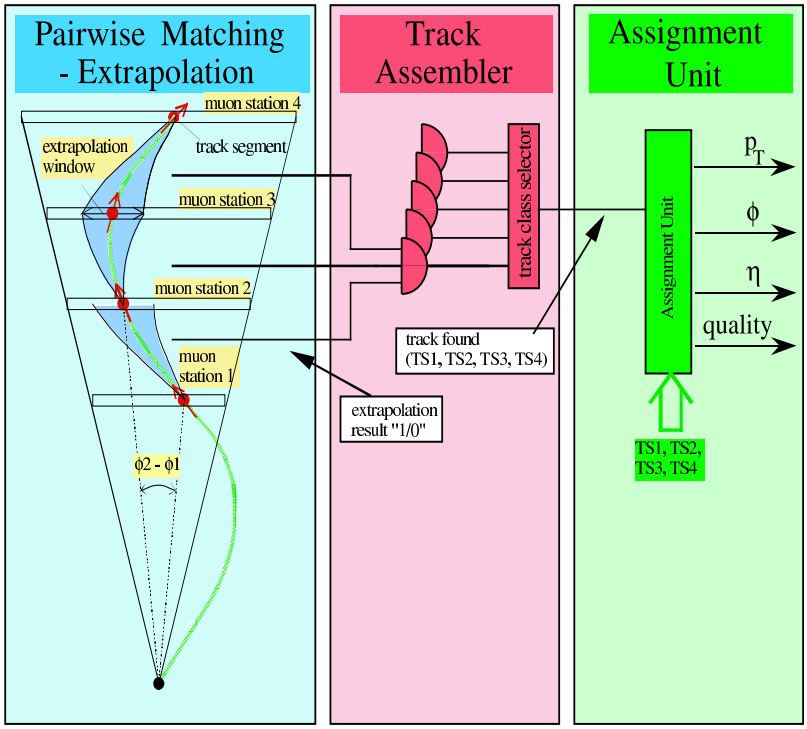

Figure 3: A scheme of the logical processes of the DT Track Finder algorithm.

3 The Drift Tubes Track Finder Trigger

A detailed description of the DTTF trigger system can be found in [3]. The task of the DTTF is to find muon tracks in the barrel region originating from the interaction point, and to measure at the hardware level their transverse momenta and their location in pseudorapidity η and azimuthal angle ϕ. This is achieved by using the trigger primitives delivered by the DT system. The DTTF reconstructs muon candidates by matching track segments from different stations, originating from the same particle which traversed the muon detector. After the track finding process, the DTTF system assigns a transverse momentum, ϕ and η coordinates, and a quality word to the muon track candidates. Finally the wedge sorter and the barrel sorter select the four highest transverse momentum tracks in the barrel detector and forward them to the global muon trigger.

The main input data stream of the ϕ DTTF system are the DT track segments that come from the sector collector units, which are the devices which collect the trigger data from the chambers of a muon sector. For each BX a maximum of two trigger segments per station can be delivered by the local trigger to the DTTF , which then attempts to construct track candidates by matching the segments from each muon station as sketched in figure 2 and 3. The DT trigger system sends all data bits of one track segment in each BX. This can be the track segment that belongs to the bunch crossing determined by the standard latency scheme, or it can be a second track segment related to the previous BX, as the local trigger can deliver up to two ϕ segments for any BX.

The DTTF algorithm can be described as a three-steps process, as shown in figure 3. First the extrapolation unit of the sector processor tries to match track segment pairs of distinct muon stations, using a pairwise matching method. This is performed by extrapolating to the next station from a track segment, using the spatial and angular measurement ϕ and ϕ_b of the track segment previously defined. The matched pairs are then forwarded to the track assembler unit, which links the segment pairs to full tracks. The assignment unit performs the last step, determining the track parameters for each trigger candidate.

4 Experimental Set-Up and Collected Data

The experimental set-up at the test beam consisted of two DT barrel muon chambers arranged as in figure 4, where the top view is shown. The whole system was installed in the H2 zone of the CERN SpS North Area and exposed to a secondary muon beam with momenta varying from 30 to 300 GeV/c. The test was carried out in October 2004, using a SpS radio frequency structure similar to the one foreseen at the LHC. The proton beam delivered by the SpS hit a primary target in narrow bunches (about 2 ns long, separated by 25 ns) generating muons. From these

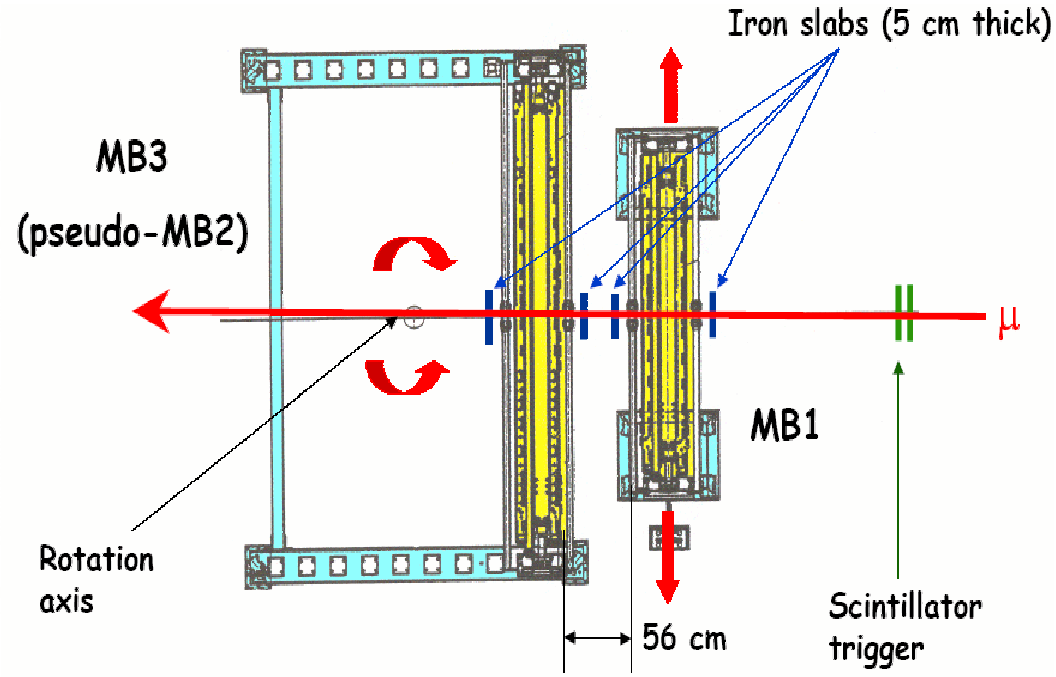

Figure 4: A top-view sketch of the experimental set-up. The muon beam direction is shown by the arrow. The bending of the muon track in the CMS magnetic field was simulated by rotating MB3, with the rotation axis orthogonal to the plane of the figure. MB1 could be shifted orthogonally to the beam direction, as shown by the arrows.

muons a secondary beam with the same time structure of the proton primary beam was formed, by selecting the proper particle momentum. Trains of 48 bunches occurred every 25 μs during a spill of 2.2 s length (a so called slow-extraction cycle of the SPS). Since a secondary beam was used, the mean muon occupancy in a bunch was rather low, of the order of 10^{-2} - 10^{-3} , and therefore muons were separated in time by several microseconds on average. The 40 MHz signal, synchronous with the accelerator RF signal, was distributed in the experimental area via a TTC system [6] through optical links, and it was used as clock signal for the readout and trigger electronics. Both chambers had the ϕ view wires in the vertical direction. The up-stream chamber with respect to the muon beam was an MB1 type chamber. It was placed on a support which allowed lateral displacement in the direction perpendicular to the beam direction, and parallel to the ground floor. The down-stream chamber was an MB3 type chamber, placed on a mechanical support which allowed rotation around its central vertical axis, as well as any horizontal displacement. A proper rotation and displacement of the MB3 chamber with respect to MB1 allowed to simulate the bending of the muon tracks in the CMS magnetic field. Both chambers were equipped with minicrates with the related read-out and trigger electronics. The trigger electronics was configured mocking an MB2 type station for MB3. Therefore, from the point of view of the trigger, an MB1 and an MB2 muon stations of the central wheel of the CMS detector were tested. The chambers were flushed with an Ar/CO_2 (85%/15%) gas mixture with a gas flow of 2 l/min. The oxygen concentration was measured by an oxygen monitor placed downstream before the gas exhaust and was always below 100 ppm during data taking. The high voltage values of the electrodes were: V_{wire} = 3600 V, V_{strip} = 1800 V, $V_{cathode}$ = -1200 V. The discrimination threshold of the front-end readout

electronics was set to 15 mV, corresponding to about 4.5 fC. Such values were those foreseen for operation at the LHC.

In order to simulate the effect of the material in the CMS muon detector, two iron slabs of 5 cm thickness each, were placed between the two stations. Two additional 5 cm thick iron slabs were installed, one in front of MB1, and one behind MB3, the latter to simulate back-scattering. Concrete blocks were located about 40 cm up-stream the two trigger scintillators during the whole data-taking.

Each of the two DT chambers delivered its local trigger data to a prototype of the trigger DT sector collector VME board. At the sector collector level the trigger data were reduced (i.e. null tracks were rejected), synchronized and fanned out to both a pattern unit [7] and to a prototype of the ϕ DTTF processor. The local DAQ acquired the trigger data from the pattern unit. The DTTF delivered its trigger track candidates to a prototype of the DT wedge sorter board, whose data output was recorded in a second pattern unit and read out via the DAQ. Two track candidates for each BX were delivered as output by the whole system. The trigger electronics system used in the test beam had prototypes of all the constituents of the CMS DT trigger system, with the exception of optical links from the sector collector to the DTTF: however, those links do not perform any processing, and optical transmission was thoroughly tested independently.

An external beam trigger was given by the coincidence of two plastic scintillators defining a 10x10 cm^2 area and almost fully covering the muon beam. Details of the electronics and data read-out system of the experimental set-up can be found in [4]. During the data taking, the hardware of the local trigger was set-up with the default configuration expected at LHC. Data were collected scanning different inclination angles of the MB3 type chamber, from -30 to +30 degrees, in steps of 10 degrees. The effect of the material placed between the two stations was studied using data collected with and without the iron absorbers, and at different muon beam momenta, in the range from 50 to 300 GeV/c. These subsets of data were collected with beam at normal incidence.

An emulation of the trigger performance was used, whose characteristics were already described in [4]. The code which simulates the trigger is the one released in the official CMS reconstruction code. For this purpose a dedicated interface was developed, which generates trigger input signals from the drift times recorded by the TDCs on the read-out boards. Such signals are then sent as input to the emulator, to check the trigger response on an event-by-event basis.

5 Experimental Results

In this section the experimental results on the performance of the trigger system obtained in the test will be described. The ideal behaviour corresponds to a high trigger efficiency, a correct identification of the BX, and a very low ghost rate. The system must also deliver the reconstructed trigger segments at the expected position and bending angle. Ghosts are copies of the trigger segment at the correct BX, as well as fake triggers at the wrong BX. They typically show-up as low quality segments in a single DT superlayer, as they may originate from a wrong alignment of hits in a DT muon station, due to the presence of extra hits produced by electromagnetic cascades and δ-rays, or from redundancies in the trigger electronics. Such features can be accurately tested by selecting events with single muons crossing the experimental apparatus at different incident angles. Results with and without the iron absorber placed between the two chambers, and as a function of the beam momentum will be shown below. If two muons cross the detector, each station is expected to deliver two trigger segments at the correct BX, both having the correct characteristics of the muon tracks. This can be tested by selecting events with two muons crossing the detector at the same beam shot. Unfortunately such events are only a small fraction of the collected data, and therefore the precision of the measurements is limited by statistics.

The DTTF system has to match the trigger segments delivered by the two muon stations in the proper way, and produce a track. It also has the task to suppress, at its output, the ghosts produced by the single muon stations at the wrong BX, still keeping high efficiency for segment matching at the correct BX. The performance of the DTTF was tested using single muon events.

The present version of the emulation code is able to reproduce data in an excellent manner, as already published in [4]. In the measurements described in this note, some of the θ BTIs were masked during the data taking, due to a configuration error. This caused the unwanted suppression of uncorrelated low quality triggers in the corresponding ϕ view of the system. For simplicity, this problem will be called the "θ BTIs problem" in the rest of this note. The emulation, in its default version, does not include such wrong BTI configurations, thus making a direct comparison with the data difficult. Only some small sets of data, corresponding to some representative data-taking conditions, were emulated including the "θ BTIs problem" in the simulation code, to test the agreement with the data. For

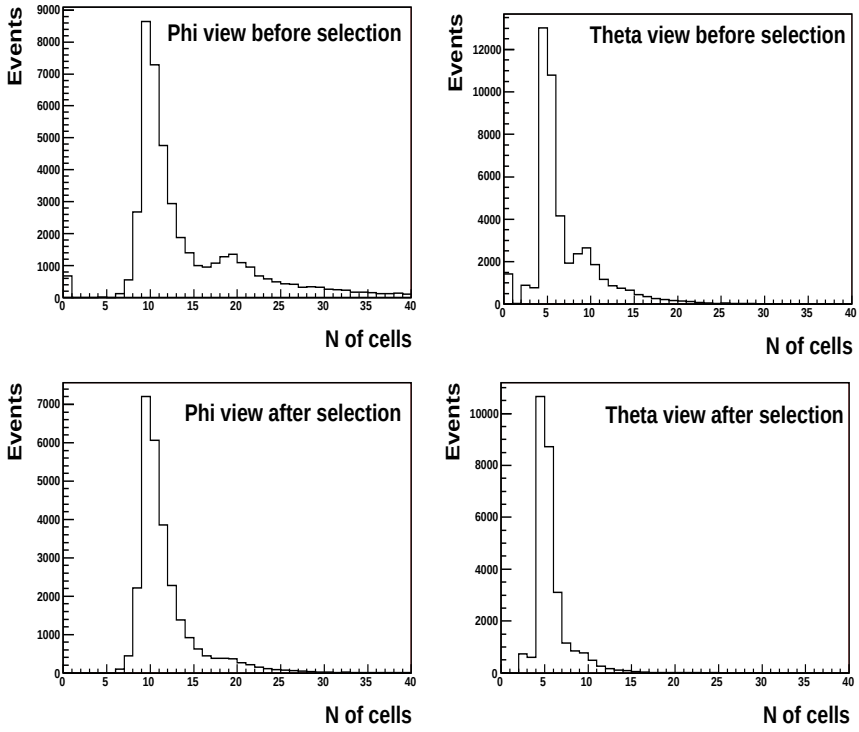

Figure 5: Distribution of the number of cells with hits in the ϕ view of the MB3 chamber (left column) and in the θ view before (top plots) and after (bottom plots) the single muon selection. The cuts of the single muon selection are performed on the quantities related to the MB1 chamber.

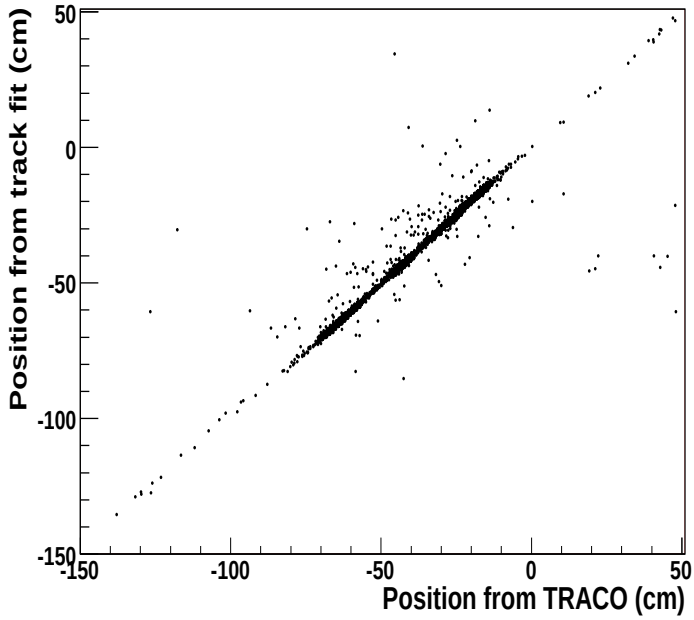

Figure 6: Correlation between the position of the track in the muon station, determined by the fit to the TDC hits (vertical axis), and the position of the trigger segment measured by the local trigger (horizontal axis).

such sets of data, results are reported in tables 1,2,3,4,5 and 6, and they show an excellent agreement between trigger data and trigger emulation. The small disagreement, observed especially in the case of out-of-time BX[2)], comes from the fact that the trigger algorithm is not emulated in the whole time range of the electronics, to keep CPU time short. In addition, some TDCs in MB3 were badly configured, which causes data coming from that part of the chamber not to provide a correct emulation of the trigger output. All the plots included in this note are obtained by summing up data from the whole set of runs taken with the same specific conditions, and for them the emulation comparison is not available. Nevertheless, in view of the excellent agreement between trigger data and trigger emulation observed in the dedicated runs, a good agreement is expected also for the whole data set.

As the trigger to the DAQ was given by the coincidence of two plastic scintillators, any selected event was required to have a signal in this device within a time window of $\pm$ 2 ns from the expected peak position.

5.1 Drift Tubes Local Trigger Results

5.1.1 Single Muon Events

Single muon events were selected by applying the selection cuts in the MB1 station, which was up-stream with respect to the beam, allowing to use the MB3 station to study the trigger performance in an unbiased manner. The quantity $\mathrm{t_0}$ is defined as the TDC time corresponding to hits issued by tracks crossing the drift tube at the wire position. The presence in the events of recorded TDC hits within a 500 ns time window after $\mathrm{t_0}$ on at least two cells, in the region of the ϕ view of MB1 illuminated by the beam, was required in order to reject events with fake scintillator coincidence.

The BTI has a programmable dead time that protects the computations in case of multiple hits on the same cell (due to afterpulses, electromagnetic background or multiple beam tracks). The first detected hit on each BTI channel raises a flag that rejects signals from late hits within a programmable time window (by default set equal to the maximum drift time $\mathrm{T_{max}}$). Therefore only hits detected in the range $-\mathrm{T_{max}} < \mathrm{t_0} < 2\mathrm{T_{max}}$ may affect the BTI calculations: hits arriving before the good one will mask it modifying the trigger decision, while hits coming afterwards will restart the BTI calculations adding noisy triggers. Therefore one can clean the sample of events with out-of-time muons by asking for less than three hits outside this time window in the ϕ view of the MB1 chamber, without introducing any bias. For this purpose, $\mathrm{T_{max}}$ was approximated to 400 ns.

A relevant number of events with two muons are still left in this selection, mainly due to the large time window allowed. To improve the single muon selection, the counting of the number of cells with hits recorded in the TDCs, falling in the selection time window, was employed. Events were discarded if more than six cells with hits in any of the three SLs were found (to reject events with two muons hitting the same tube). The impact of the selection on the normal incidence sample is shown in figure 5 where the distributions of the number of cells with hits for all the events (top row) and for selected events (bottom row) in the ϕ view (left column) and in the θ view (right column) of MB3 are shown. Similar results hold at any angle of incidence. In summary, the single muon event selection cuts were the following:

- scintillator trigger time with $\pm$2 ns tolerance around the average time
- at least 3 cells with recorded hits in the beam region, in the ϕ view of MB1, with recorded TDC time within 500 ns from the $\mathrm{t_0}$ of the event
- less than 3 hits recorded outside the time interval range $-400 < \mathrm{t_0} < 800$ ns in the ϕ view of MB1
- a maximum of 6 cells with hits in every SL of MB1

Typically about 65 $\%$ of the triggered events pass the single muon selection cuts. A different single muon event selection was also tested, to check the presence of bias in the event selection. Events were required to have a HH trigger segment in MB1 at the correct BX, and exactly 8 cells with hits in the ϕ view of the same station. Such requirements are more stringent than the ones listed above, and in principle should allow to select a cleaner sample of isolated muons crossing the experimental set-up at the correct time. Nevertheless, no relevant systematic differences are observed in the experimental results when the two selections are compared.

TDC hits were fitted by the CMS reconstruction program, which was specially adapted for the test beam data. Fitted track segments resulting from aligned TDC hits were found in each muon chamber separately, and independently

[2)] Trigger segments which are not assigned to the correct BX are called "out-of-time" triggers.

Muon momentum = 150 GeV/c, angle = -10 degrees, no iron absorber				
Triggers at correct BX (%)				
Trigger type	Data 1st track	Emulation 1st track	Data 2nd track	Emulation 2nd track
HH	65.7	65.7	0.5	0.4
HL	18.2	18.2	0.7	0.6
LL	5.0	5.0	1.1	1.1
H_o	3.1	3.1	0.5	0.7
H_i	5.6	5.6	1.5	1.4
L_o	0.2	0.1	0.7	0.4
L_i	0.4	0.3	1.0	0.5
Total	98.1	98.0	6.1	5.1
Triggers at "out-of-time" BX (%)				
HH	1.3	0.2	0.02	-
HL	1.0	0.5	0.03	0.01
LL	4.4	4.4	0.05	0.03
H_o	5.6	5.0	0.02	0.01
H_i	4.9	4.6	0.04	0.02
L_o	6.4	7.6	0.5	0.6
L_i	10.1	12.0	0.9	0.9
Total	33.7	34.3	1.6	1.6

Table 1: Breakdown of the DT local trigger segment quality in single muon events, obtained from a run with beam momentum equal to 150 GeV/c beam incident angle of -10 degrees, and no iron absorber placed between the two stations. Data and emulator trigger results are both reported, for correct and "out-of-time" BX identification.

Muon momentum = 150 GeV/c, angle = -30 degrees, no iron absorber				
Triggers at correct BX (%)				
Trigger type	Data 1st track	Emulation 1st track	Data 2nd track	Emulation 2nd track
HH	68.3	67.7	0.8	0.6
HL	15.2	15.4	0.6	0.6
LL	0.9	0.9	0.1	0.1
H_o	5.3	5.3	1.0	1.0
H_i	8.0	8.2	2.1	1.9
L_o	0.1	0.1	0.5	0.4
L_i	0.3	0.2	0.8	0.4
Total	98.1	97.9	5.8	4.9
Triggers at "out-of-time" BX (%)				
HH	1.5	0.4	0.03	-
HL	1.7	1.6	0.01	0.01
LL	3.1	3.3	0.04	0.03
H_o	8.5	8.7	0.04	0.02
H_i	8.6	8.3	0.08	0.02
L_o	8.3	9.1	0.7	0.7
L_i	10.7	11.1	0.9	0.8
Total	42.5	42.5	1.7	1.6

Table 2: Breakdown of the DT local trigger segment quality in single muon events, obtained from a run with beam momentum equal to 150 GeV/c beam incident angle of -30 degrees, and no iron absorber placed between the two stations. Data and emulator trigger results are both reported, for correct and "out-of-time" BX identification.

Muon momentum = 100 GeV/c, angle = 0 degrees, no iron absorber				
Triggers at correct BX (%)				
Trigger type	Data 1st track	Emulation 1st track	Data 2nd track	Emulation 2nd track
HH	67.2	67.1	0.3	0.3
HL	14.6	14.7	0.4	0.4
LL	1.0	1.0	0.1	0.1
H_o	4.6	4.6	0.5	0.5
H_i	7.0	7.0	1.4	1.4
L_o	0.3	0.3	0.3	0.3
L_i	0.5	0.5	1.0	0.8
Total	95.1	95.1	4.1	3.8
Triggers at "out-of-time" BX (%)				
HH	1.4	0.4	0.02	-
HL	1.0	0.6	0.01	-
LL	7.5	7.4	0.06	0.05
H_o	4.1	3.9	0.03	0.01
H_i	3.3	3.2	0.08	0.02
L_o	7.9	7.9	0.5	0.4
L_i	11.4	11.1	1.6	1.4
Total	36.6	34.4	2.3	1.9

Table 3: Breakdown of the DT local trigger segment quality in single muon events, obtained from a run with beam momentum equal to 100 GeV/c orthogonal beam angle, and no iron absorber placed between the two stations. Data and emulator trigger results are both reported, for correct and "out-of-time" BX identification.

Muon momentum = 100 GeV/c, angle = 0 degrees, with iron absorber				
Triggers at correct BX (%)				
Trigger type	Data 1st track	Emulation 1st track	Data 2nd track	Emulation 2nd track
HH	62.3	62.4	0.2	0.2
HL	15.2	15.0	0.5	0.5
LL	1.1	1.1	0.2	0.1
H_o	6.8	6.8	0.7	0.7
H_i	7.5	7.6	1.5	1.5
L_o	0.5	0.5	0.4	0.4
L_i	0.8	0.7	1.6	1.1
Total	94.1	94.1	5.0	4.5
Triggers at "out-of-time" BX (%)				
HH	1.8	0.6	0.02	0.01
HL	1.7	1.4	0.02	0.01
LL	9.2	8.9	0.1	0.1
H_o	6.0	5.8	0.05	0.03
H_i	7.2	7.0	0.14	0.07
L_o	9.8	10.2	0.8	0.8
L_i	19.1	19.0	2.7	2.6
Total	54.8	52.7	3.9	3.6

Table 4: Breakdown of the DT local trigger segment quality in single muon events, obtained from a run with beam momentum equal to 100 GeV/ c orthogonal beam angle, and with the iron absorber placed between the two stations. Data and emulator trigger results are both reported, for correct and "out-of-time" BX identification.

Muon momentum = 300 GeV/c, angle = 0 degrees, no iron absorber				
Triggers at correct BX (%)				
Trigger type	Data 1st track	Emulation 1st track	Data 2nd track	Emulation 2nd track
HH	67.1	67.1	0.4	0.4
HL	14.6	14.5	0.3	0.4
LL	0.9	0.9	0.1	0.1
H_o	4.4	4.4	0.5	0.6
H_i	6.9	6.9	1.6	1.5
L_o	0.2	0.2	0.3	0.3
L_i	0.4	0.4	0.8	0.6
Total	94.4	94.4	4.0	3.8
Triggers at "out-of-time" BX (%)				
HH	1.0	0.3	0.02	-
HL	0.9	0.6	0.01	-
LL	7.1	6.8	0.05	0.03
H_o	4.7	4.6	0.02	0.01
H_i	3.6	3.5	0.07	0.01
L_o	6.9	6.9	0.5	0.5
L_i	9.0	9.5	1.2	1.0
Total	33.1	32.2	1.8	1.5

Table 5: Breakdown of the DT local trigger segment quality in single muon events, obtained from a run with beam momentum equal to 300 GeV/c orthogonal beam angle, and no iron absorber placed between the two stations. Data and emulator trigger results are both reported, for correct and "out-of-time" BX identification.

Muon momentum = 300 GeV/c, angle = 0 degrees, with iron absorber				
Triggers at correct BX (%)				
Trigger type	Data 1st track	Emulation 1st track	Data 2nd track	Emulation 2nd track
HH	59.5	59.5	0.2	0.2
HL	14.8	14.9	0.3	0.4
LL	1.5	1.4	0.1	0.1
H_o	7.8	7.7	0.7	0.8
H_i	7.6	7.7	1.9	1.8
L_o	0.6	0.6	0.4	0.4
L_i	0.9	1.0	1.5	1.2
Total	92.6	92.7	5.2	4.8
Triggers at "out-of-time" BX (%)				
HH	1.3	0.8	0.01	0.01
HL	2.4	2.2	-	0.03
LL	9.7	9.4	0.1	0.09
H_o	7.8	7.7	0.06	0.03
H_i	9.7	9.5	0.1	0.08
L_o	9.4	9.7	0.8	0.9
L_i	20.7	20.8	2.9	2.6
Total	60.9	59.9	4.0	3.7

Table 6: Breakdown of the DT local trigger segment quality in single muon events, obtained from a run with beam momentum equal to 300 GeV/c orthogonal beam angle, and with iron absorber placed between the two stations. Data and emulator trigger results are both reported, for correct and "out-of-time" BX identification.

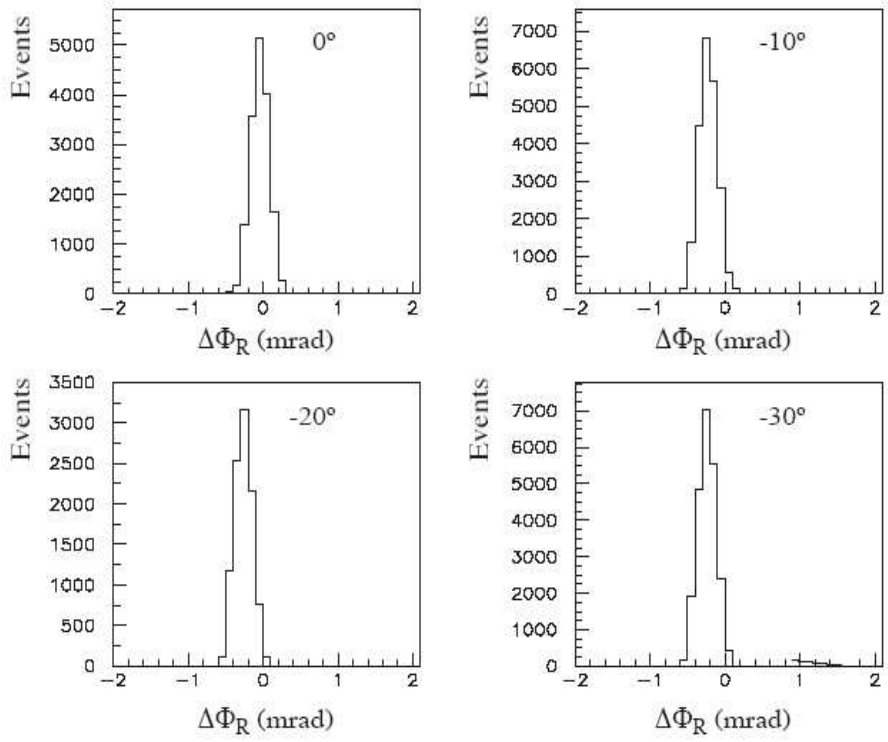

Figure 7: Distribution of the quantity $\Delta\Phi_{\rm R}$, defined as the difference between the radial angle ϕ determined by the trigger segment, and the radial angle determined by the fit to the TDC hits. The plots are obtained using HH type trigger segments only, and are shown for different beam inclinations. The variance of the quantiity $\Delta\Phi_{\rm R}$ is about 0.150 mrad. Results are similar also for uncorrelated triggers.

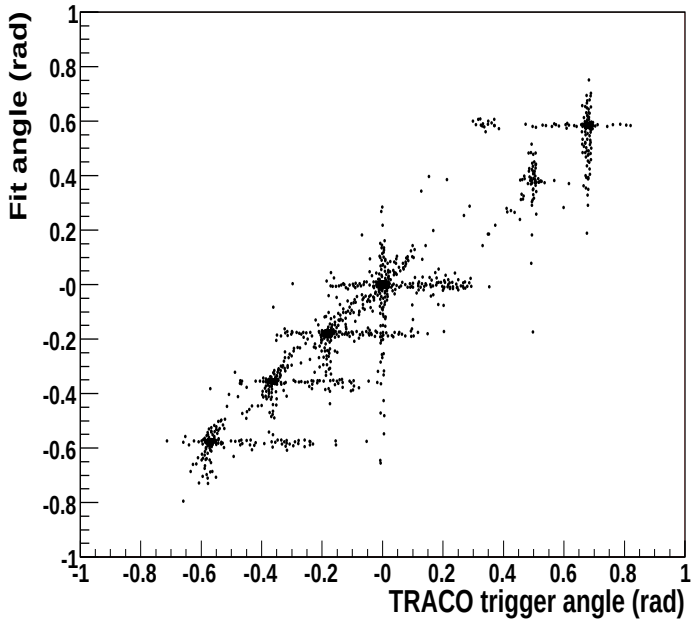

Figure 8: Correlation between the incident angle determined by the fit to the TDC hits (vertical axis) and the incident angle of the trigger segment ϕ_b (horizontal axis).

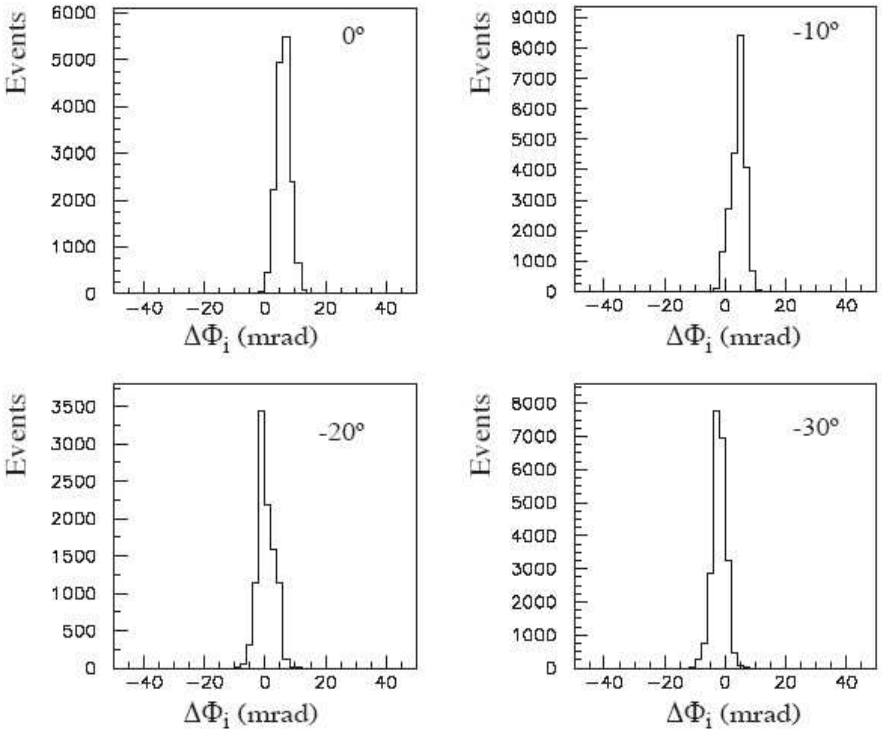

Figure 9: Distribution of the quantity $\Delta\Phi_{\rm i}$, defined as the difference between the incident angle ϕ_b of the trigger segment in MB3, and the radial angle determined by the fit to the TDC hits. The plots are obtained using HH type trigger segments only, and are shown for different beam inclinations. The variance of the quantity $\Delta\Phi_{\rm i}$ is between 2 and 3 mrad, and about a factor of 10 larger for uncorrelated triggers.

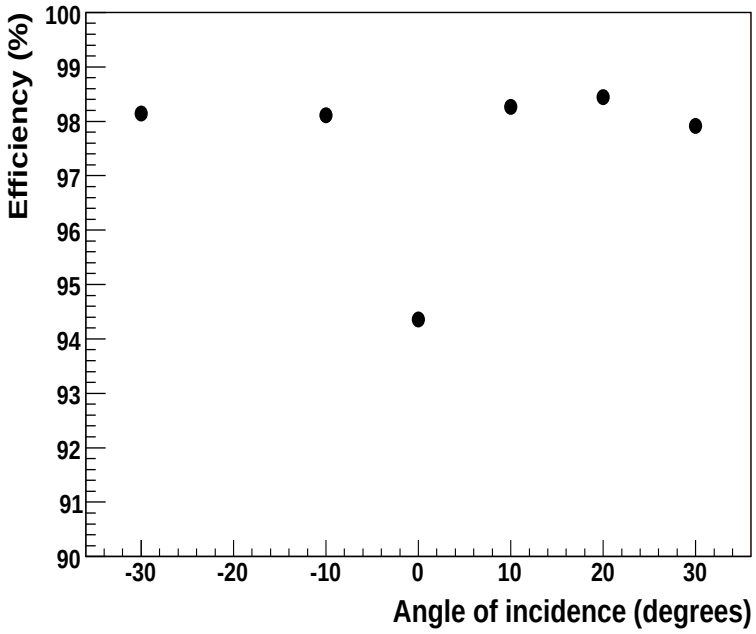

Figure 10: BX identification efficiency in MB3 for single muon events, as a function of the particle incident angle.

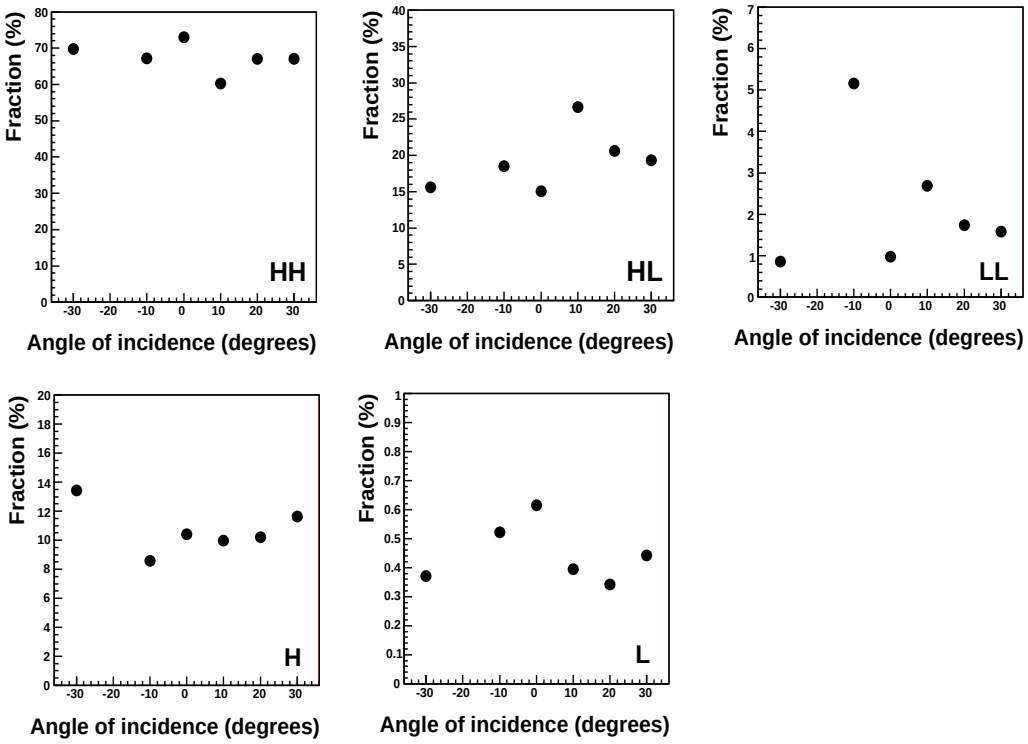

Figure 11: The fractions of trigger segments in each quality category, for the MB3 chamber, as a function of the particle incident angle. Point to point fluctuations are mainly due to the different impact point of the beam in the chamber, as explained in the text.

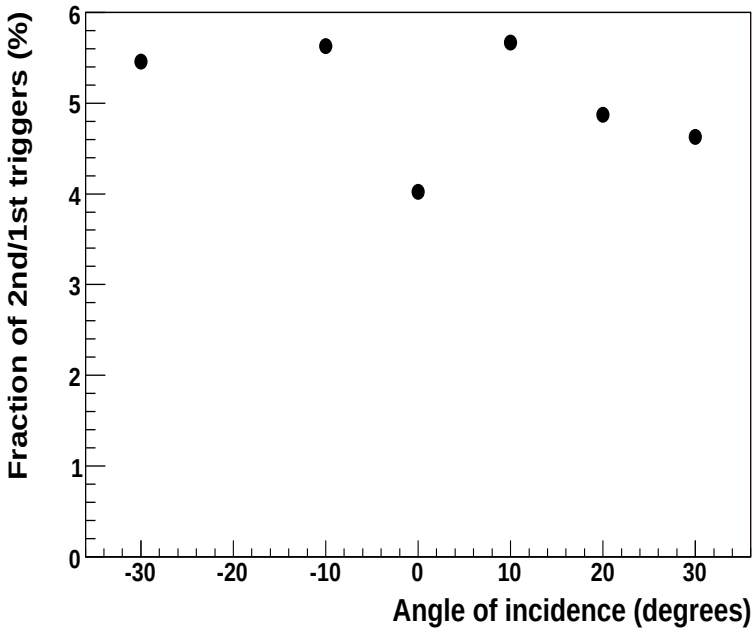

Figure 12: Fraction of ghost triggers observed in MB3, defined as the ratio of the number of second tracks over the number of first tracks, delivered by the local trigger at the correct BX, as a function of the beam incident angle, for single muon events.

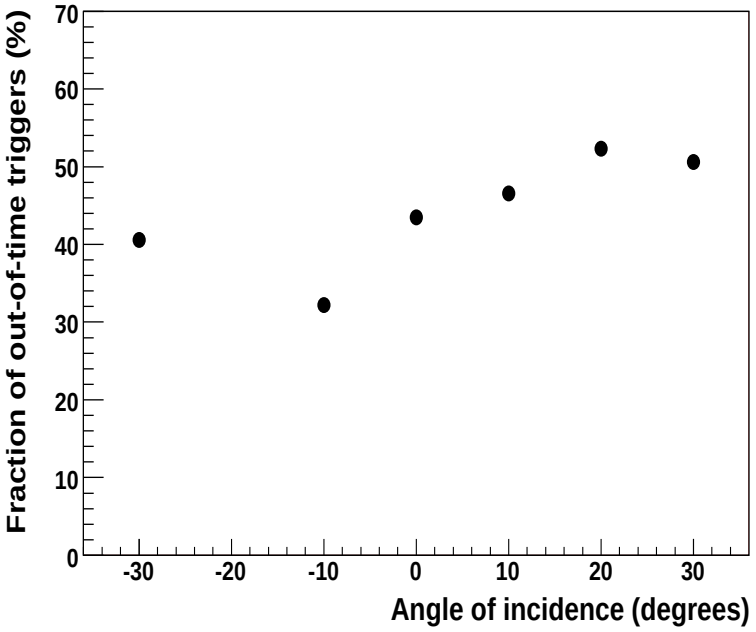

Figure 13: The fraction of out-of-time triggers per event observed in MB3, defined as the total number of such triggers divided by the number of in-time triggers, as a function of the beam incident angle. The value of 50 % looks high but measurements discussed in section 5.2 show that the ghosts at the output of the local trigger are almost entirely killed by the DTTF.

from the local trigger results. Figure 6 shows the correlation between the position of the track in MB3, measured by the fit to the TDC hits, and the position of the trigger segment determined by the local trigger (the quantity previously defined as the radial angle ϕ, here expressed in centimeters to identify the position of the trigger segment in the muon station). The radial angle resolution for different beam incident angles is shown in figure 7 for HH type triggers. Similar results are also obtained with trigger segments having a lower quality. The variance of the distributions is about 0.150 mrad, and the shift of the average from the zero of the distributions is about 0.250 mrad, not depending on angle, except for normal incidence. This might be interpreted a systematic uncertainty due to the reference system.

Data were taken at different incident angles in the MB3 chamber. The correspondence between the nominal beam incident angle and the incident angle determined by the trigger segment is shown in figure 8. The distribution of the incident angle ϕ_b of the HH type trigger segments, subtracted by the corresponding quantity as determined by the track fit, is shown in figure 9 for different incident angles. The variance, which can be interpreted as the ϕ_b resolution, is about 2-3 mrad, whereas for uncorrelated triggers it is about 30 mrad.

The BX identification efficiency is defined as the fraction of selected single muon events for which the local trigger delivered at least one trigger segment at the correct BX, and it is shown in figure 10 as a function of the beam incident angle. The lower efficiency at 0 degrees, already observed in [4], is a geometrical effect due to the staggering of the drift cells. Due to the θ BTIs problem described before, the overall BX identification efficiency is about 2 $\%$ lower than what was obtained in the default configuration, already published in [4]. This is mainly due to the fact that about 2 $\%$ of uncorrelated low quality trigger segments are lost. The breakdown of the trigger quality, when the correct BX is identified, is shown in figure 11, as a function of the beam incident angle. Point to point fluctuations are explained by the variation of the impact point of the beam on the chamber, as for any given inclination of the incoming muon track, the fraction of correlated and uncorrelated track segments slightly depends on the position of the track itself in the TRACO unit.

In the case of single muon events, if two trigger segments are delivered at the same BX by the local trigger system in a muon station, the second trigger is considered a ghost copy of the first one. Although generally with a poorer quality, ghosts at the correct BX reproduce the characteristics of the main trigger segment in terms of position and angle. Figure 12 shows the fraction of ghost triggers per event, defined as the fraction of single muon events with two triggers at the correct BX in MB3, as a function of the beam incident angle.

When the DT local trigger associates a wrong BX to a hit alignment, so called ”out-of-time” ghosts are produced.

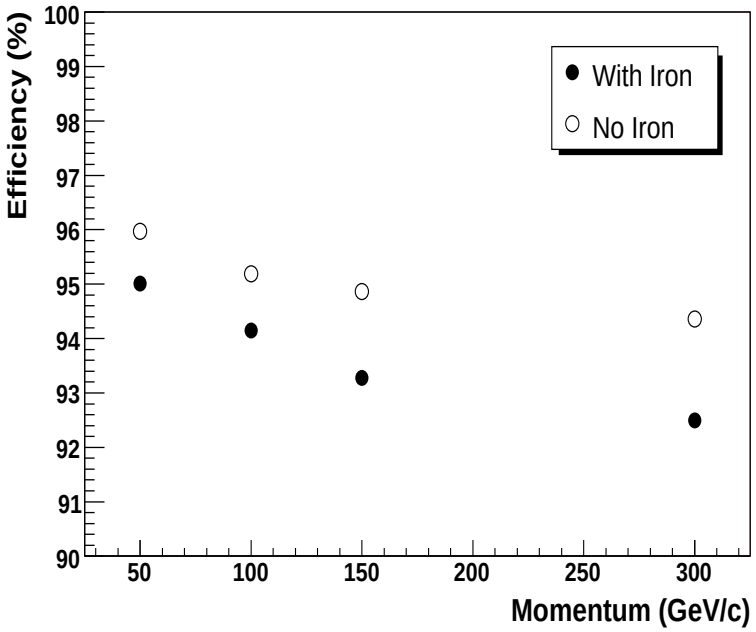

Figure 14: BX identification efficiency in MB3 as a function of the incident muon momentum, for events with and without the iron absorber placed in front of MB3.

In figure 13 the measured fraction of out-of-time triggers per event is shown as a function of the beam incident angle. Such triggers are almost all uncorrelated low quality segments, where the hit alignment is spoiled by δ-ray production or electromagnetic showers, and they are distributed over a wide range of BXs. Although the number of out-of-time triggers per event is high, the test of the DTTF performance, discussed in section 5.2, shows that it is very unlikey that such segments are linked together among different stations to form a trigger candidate track. It must be pointed out that, as ghosts are preferentially single low quality segments, the θ BTIs problem already discussed makes the observed ghost rate lower than what is expected if the default BTIs configuration was used.

The effect of the iron absorber placed between the two muon stations is the enhancement of the probability for a high momentum muon to produce electromagnetic shower. Such a probability also increases as a function of the muon momentum. This has the effect to decrease the BX identification efficiency, and to increase the noise rate, and therefore to partially reduce the trigger capability of the system. The BX identification efficiency for the MB3-type station is shown in figure 14 as a function of the muon momentum, for events with and without the iron absorber. The efficiency loss as a function of the increasing momentum, in the case of no absorber in front of MB3, can only be marginally explained by the electromagnetic showers induced by the presence of the concrete block placed up-stream of the scintillator trigger device. In fact the tighter event selection described before, based on the request of a clean HH trigger segment sample in MB1, does not have any sizeable effect in changing the drop of the efficiency in MB3. Therefore we think that the loss of efficiency, even in the case of no absorber placed between the two stations, is more likely due to electromagnetic showers induced by the material in MB3 itself. Additional contributions to the small efficiency loss may arise from observed differences in the characteristics of the beam at different beam momenta, and from some small occasional variations in the synchronization of the electronics during the data taking.

From the point of view of the DTTF ϕ track finder algorithm, also trigger segments occurring at the BX adjacent to the correct one can be used to form a track trigger candidate, if a proper matching with segments at other muon stations is achieved. Therefore such trigger segments occurring at the ”wrong” BX can still contribute to the effective DTTF trigger efficiency, if they reproduce the correct inclination and position of the incident muon track. A dedicated analysis showed that, when the iron absorber is placed between the two stations, the effective efficiency of the down-stream station increases by only about 0.5 % when also such ”wrong BX” trigger segments are taken into account. This becomes only about 0.3 % in the case of no absorber.

The fractions of trigger segments in each quality category, for the MB3 chamber, as a function of the beam momentum, with and without absorber, are shown in figure 15.

The fraction of ghost triggers at the correct BX as a function of incident muon momentum, and the fraction of

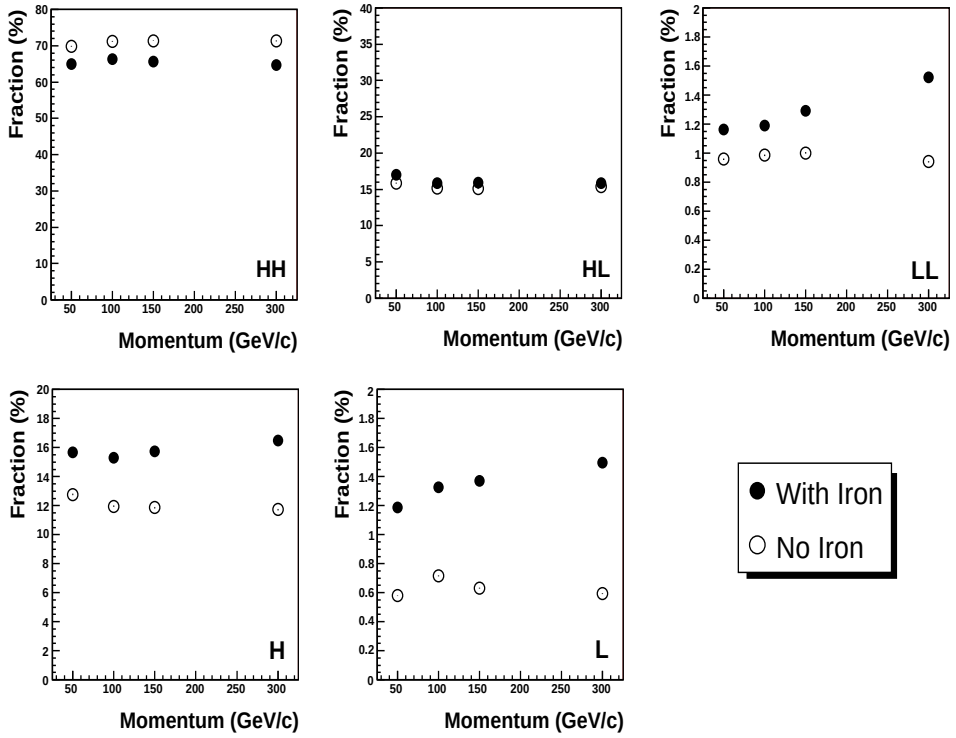

Figure 15: The fractions of trigger segments in each quality category, for the MB3 chamber, as a function of the beam momentum, for events with and without the iron absorber placed in front of MB3.

out-of-time triggers, as defined above, are shown respectively in figure 16 and 17 as a function of the incident muon momentum, for events with and without the iron absorber.

5.1.2 Two Muon Events

Events with two muons crossing the experimental set-up are not rare in the collected data sample. This can be seen in the top row of plots of figure 18, which shows the number of cells with hits in the ϕ and θ views of MB3 before any event selection. In addition to the highest peak, which is due to single muon events, the peak related to di-muon events is clearly visible. Unfortunately most of such events are due to muon pairs which belong to different beam shots (BXs), and which cross the detector separated by time intervals which are multiples of 25 ns. In order to test the trigger performance with muon pairs, the two muons must belong to the same beam shot.

Results of a test on the local trigger performance with di-muon events were published in [4]. The measurements presented in this note also include the results obtained with and without the iron absorber, as well as a different di-muon selection, less biased than what was already published in the former publication. This was possible as for the present work two separate stations were available, and the selection was performed in MB1 without affecting the performance of MB3. As for single muon analysis, muon pairs were selected in MB1, and the local trigger performance was tested in MB3. The di-muon selection cuts were the followings:

- scintillator trigger time with ± 2 ns tolerance around the average time
- a maximum of 2 cells "not in time"[3)], recorded anywhere in the ϕ view of MB1
- two trigger segments in the ϕ view of MB1, both at the correct BX, and both of quality HH. This allows to select simultaneous muon pairs which cross the experimental set-up. The two trigger segments must also be separated by more than 3 cm in space
- exactly 16 cells with at least one hit "in time" in the ϕ view of MB1. Together with the previous request, it ensures that the selected muon pair is not associated to an electromagnetic shower or a particle splash already at its origin

[3)] In this case we refer as "in time" those hits which occur in the time range $t_0 < t < t_0 + 400$ ns.

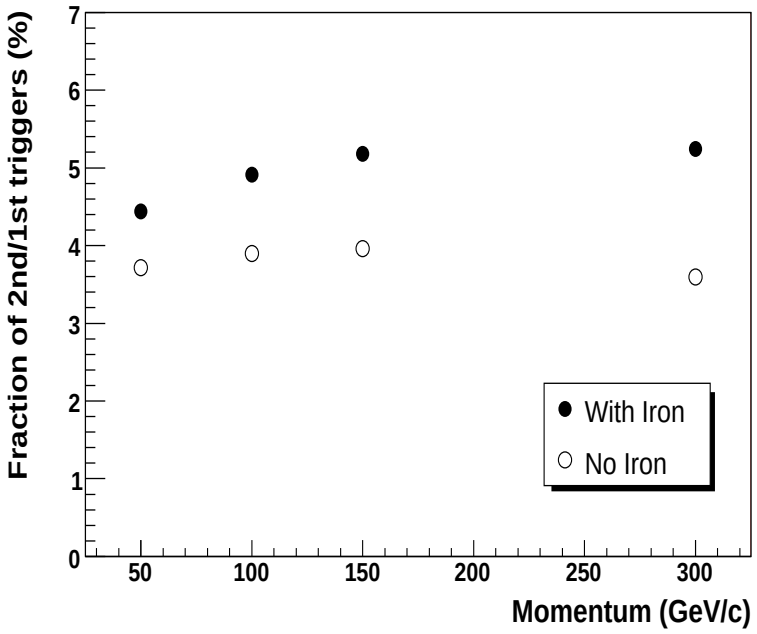

Figure 16: Fraction of ghost triggers observed in MB3, defined as the ratio of the number of second tracks over the number of first tracks, delivered by the local trigger at the correct BX, as a function of the muon momentum, for events with and without the iron absorber.

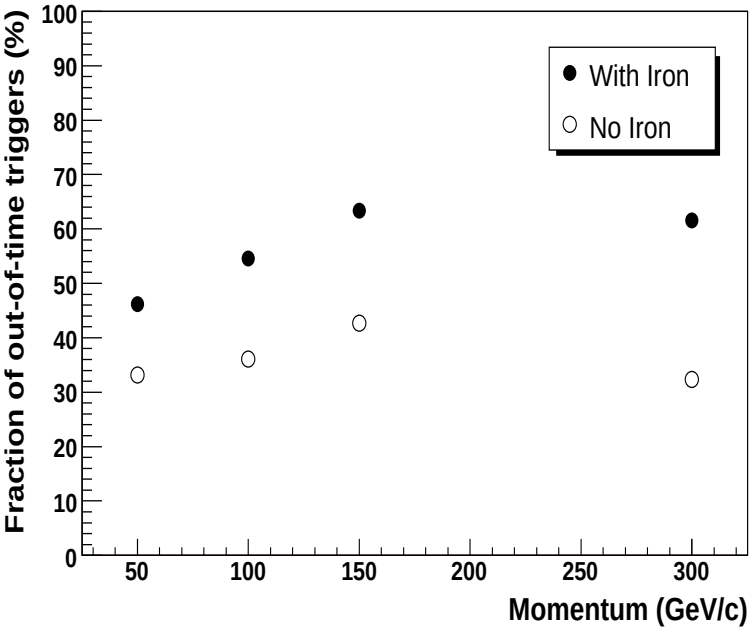

Figure 17: The fraction of out-of-time triggers in MB3, defined as the number of out-of-time trigger segments divided by the number of selected single muon events, as a function of the muon momentum, for events with and without the iron absorber.

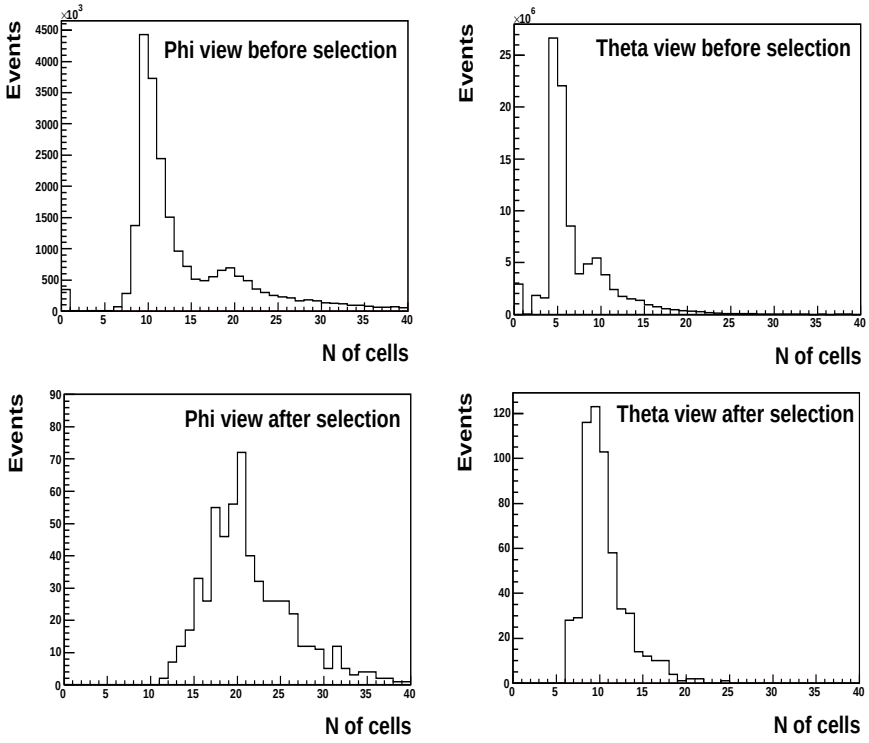

Figure 18: Number of cells with hits in the ϕ view (left column) and θ view (right column) of the MB3 muon station, before (top) and after (bottom) the di-muon event selection.

- ≥ 12 cells with at least one hit in the ϕ view of MB3, and ≥ 7 in the η view. This is the only selection cut imposed in MB3, and it is needed to remove events in which the muons do not cross the muon station in its fiducial region. This is because for some runs MB3 was shifted or tilted with respect to MB1, and therefore there was not a full overlap of the two stations
- for the few data taking runs in which TDCs were not correctly configured in some limited areas of the MB3 station, events were rejected when one of the two muons was expected to hit such areas

The plots in the bottom row of figure 18 show the distribution of the number of cells with hits in the ϕ and θ view of MB3 for events after the two-muon event selection. The fraction of di-muon selected events is less than 1 $\%$ of the triggered events, which corresponds to only a few thousand events in total. This makes the precision of the measurements performed with such events limited by statistics.

The performance of the DT local trigger, for such events, is evaluated in terms of efficiency to deliver two trigger segments either at the correct BX or one at the correct BX and the other at the nearby BX, as for the DTTF both cases provide segments to build the correct muon trigger candidate track. In addition, each of the two trigger segments must represent the corresponding muon track. This is ensured by asking that the two delivered segments are separated by more than 3 cm in MB3. Trigger segments closer in space have a high probability of being fake copies of the same muon track, and therefore, in practice, they would not contribute to the di-muon trigger efficiency.

The leftmost plot in figure 19 shows the distribution of the distance between the two muon segments found in MB1, which are used to define the di-muon sample. The distribution of the distance of the two segments when two trigger segments are also detected by the DT local trigger in MB3, both at the correct BX or in adjacent BXs, are superimposed in the same plot.[4)]

In the rightmost plot of figure 19 the di-muon trigger efficiency as a function of the distance between the two muons is shown. The efficiency is defined as the fraction of selected di-muon events which have either two trigger segments at the correct BX in MB3, or one at the correct BX and one at the adjacent BX, accordingly to the distributions shown in the leftmost plot of figure 19. All di-muon events collected during the whole data taking are

[4)] In the latter case the two segments must also correctly represent the two muons, thus being separated by more than 3 cm.

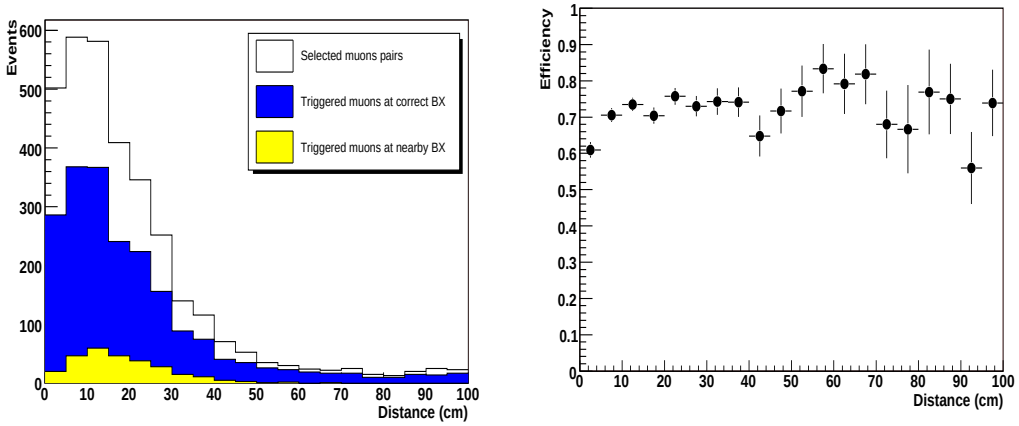

Figure 19: The distribution of the distance between the two muon trigger segments released in the MB1 station. Superimposed are the distributions when the two muons are detected also in MB3 at the correct BX (dark grey or blue) or at the adjacent BX (light grey or yellow). The plot on the right shows the efficiency to detect two muons at the correct BX or at the adjacent BX, as a function of the distance between the two muons.

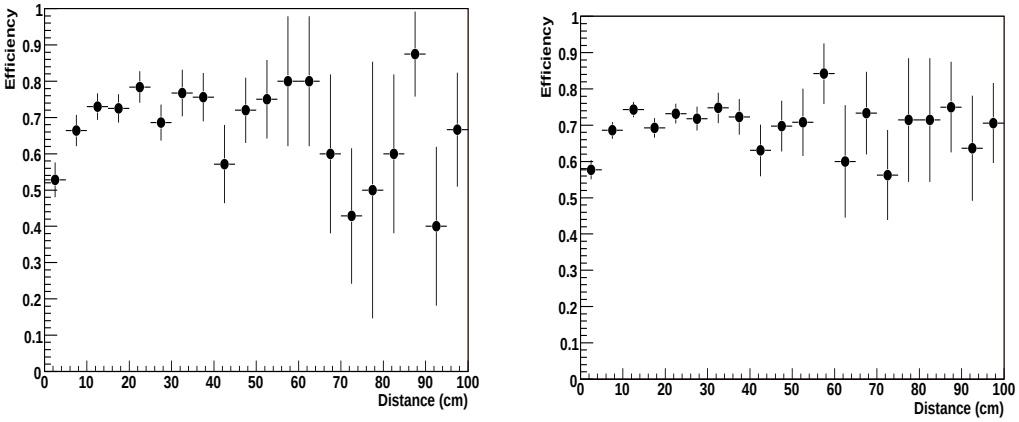

Figure 20: The di-muon efficiency in MB3, as defined in the main text, as a function of the distance between the two muons, with and without the iron absorber placed in front of MB3 (plot on the left and plot on the right respectively).

included in the plot.

The efficiency is about 60 - 70 % when the two tracks cross the detector within about 20 cm (roughly the size covered by one TRACO unit), as in such cases the ghost suppression mechanism together with the vicinity of the trigger segments may cause a loss of potentially good tracks. When the two tracks are more separated in space, the efficiency reaches a plateau at its full value. Unfortunately, in addition to the limited di-muon statistics, most of the muon pairs were very close in space, preferentially within the beam-spot region[5)], thus not allowing a precise test of the trigger performance when the two tracks are distant in space.

The effect of the iron absorber was tested with the di-muon sample, although with lower statistical precision than for single muons. Only data with beam orthogonal to the two stations are available for this test. Figure 20 shows on the left the di-muon efficiency, as defined above, with the iron absorber between the two muon stations. The plot on the right reports the di-muon efficiency with no absorber between the stations. Data with different beam momenta are all included in the plots. Within the available statistical precision, the two plots look very similar.

The effect of a non-orthogonal incident beam is to slightly increase the BX identification efficiency with respect to orthogonal incidence, as already shown for single muon events. Figure 21 shows the local trigger di-muon efficiency, still defined as above, in the case of an orthogonal angle of incidence of the beam on the station,

[5)] In particular the beam condition was such that muons from the beam halo were fewer with respect to the test described in [4].

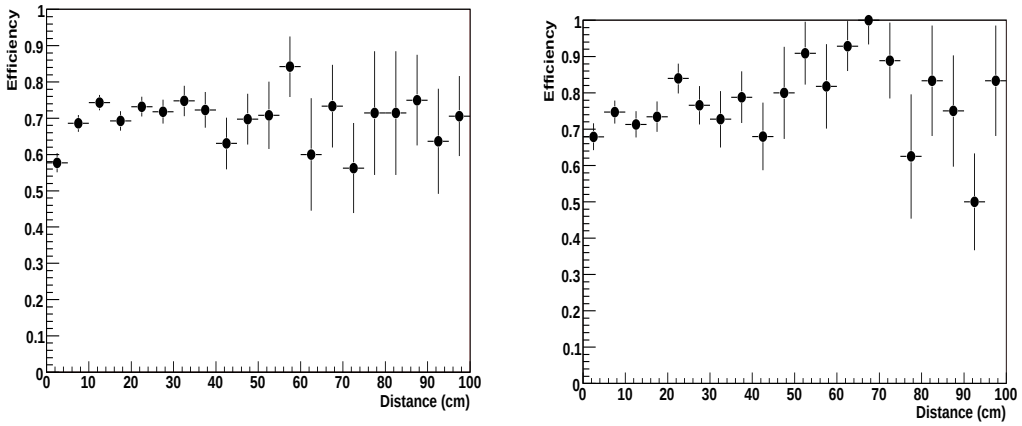

Figure 21: The di-muon local trigger efficiency, as defined in the main text, as a function of the distance between the two muons, when the beam is orthogonal to the MB3 station (plot on the left) and for angles different from zero degrees (plot on the right).

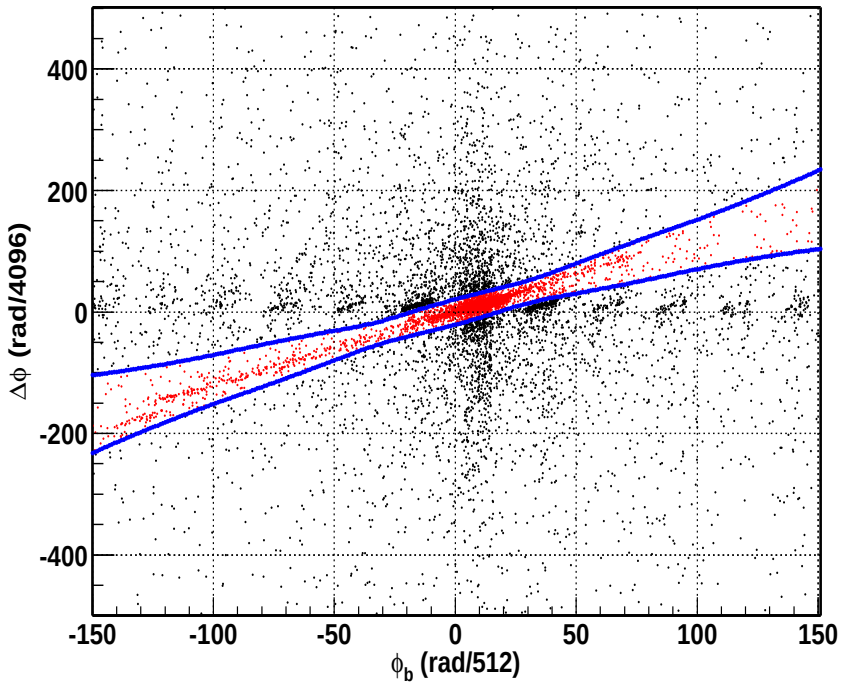

Figure 22: Difference $\Delta\phi$ between the two values ϕ_b of the trigger segment in MB1 and MB3, as a function of the value ϕ_b in MB1. The reconstructed DTTF tracks lie in the narrow band where the extrapolation is allowed, as expected. The other points are wrong associations, and are not reconstructed by the DTTF algorithm. The beam spread simulates a spread in transverse momentum.

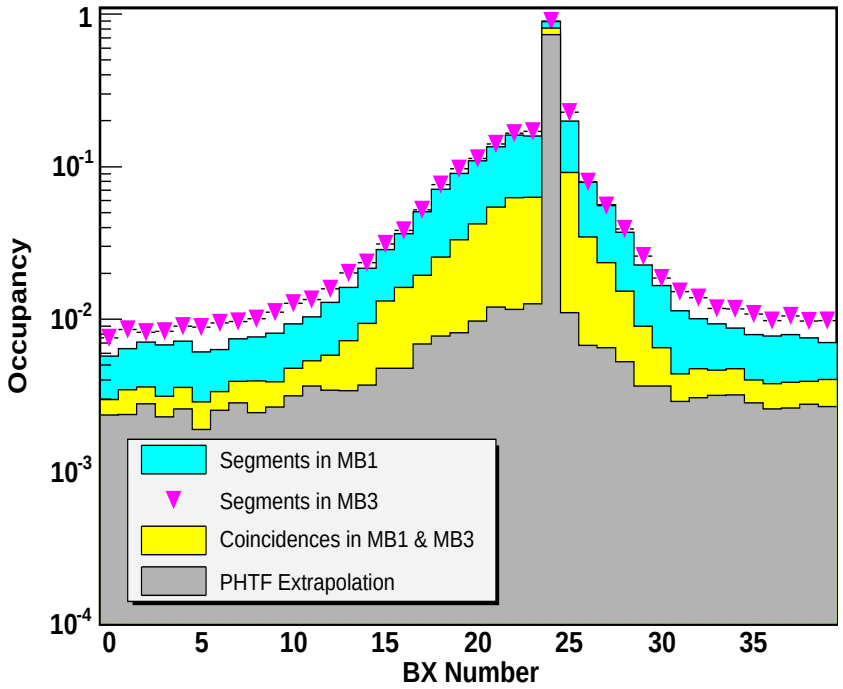

Figure 23: Distribution of the BX assigned to the tracks found by the DTTF. The BX is correctly identified when its value is 24. Superimposed are the distributions of the same quantity determined independently by the local trigger in MB1 and MB3, as well as the distribution of the determined BX when a trigger segment at the same BX was delivered in coincidence in MB1 and MB3.

and with different inclinations (all data with beam inclinations other than normal were summed). Within the limited statistical precision, the efficiency appears to be higher in the case of incident angles different from zero, as expected.

5.2 Phi Track Finder Results

In the real CMS detector, a muon track crossing the MB1 station with a given inclination and at a given point, has a well defined transverse momentum. With the present test beam set-up, muon tracks cross the MB1 station orthogonally, and their impact point is not fixed, but depends on the beam spread, which is of the order of few centimeters. Taking as a guideline figure 2, for a given impact point of the incident track in MB1, expressed by the quantity ϕ, there is a precise relation between its incident angle ϕ_b in MB1, and the expected angle ϕ_b in MB3. This holds also for the present experimental set-up. If we call $\Delta\phi$ the difference between $\phi_{\rm b}$ in MB1 and MB3, the tracks which cross the two muon stations are expected to fall within the narrow band of figure 22. Therefore, among all the possible DT trigger segments released by the two muon stations, only those which have bending angles which fall in such a band can be successfully matched by the DTTF algorithm to form a trigger track. The beam spread in this case simulates a spread of transverse momentum values. In the same figure the points which correspond to the successful extrapolations, all lie within the expected range. Other points represent all the rejected coincidences. For the analysis of the DTTF results, all the events which gave the trigger-scintillators coincidence were analyzed, without any further selection cut.

Figure 23 shows the distribution of the BX assigned to the tracks found by the DTTF. The BX is correctly identified when its value is 24. Superimposed are the distributions of the same quantity determined independently by the local trigger in MB1 and MB3, as well as the distribution of the determined BX when a trigger segment with the same BX was delivered in coincidence in MB1 and MB3. It can be seen that the DTTF is fully efficient to deliver track candidates at the correct BX, whereas for out-of-time triggers the corresponding DTTF trigger rate is suppressed at the level of 1 % or less. A large fraction of the out-of-time triggers is due to real muons crossing the experimental apparatus at a BX different from 24, and which are correctly reconstructed by the DTTF. This is confirmed by the fact that the trigger segments which are matched together to form such tracks, are mainly of the type HH, thus indicating the passage of a real muon track. Figure 24 shows the efficiency for the DTTF to reconstruct a trigger track as a function of the BX. Superimposed are the efficiency to reconstruct a trigger track when the two trigger segments are both of HH type, and both of L quality respectively. The correct BX is 24. The DTTF efficiency for

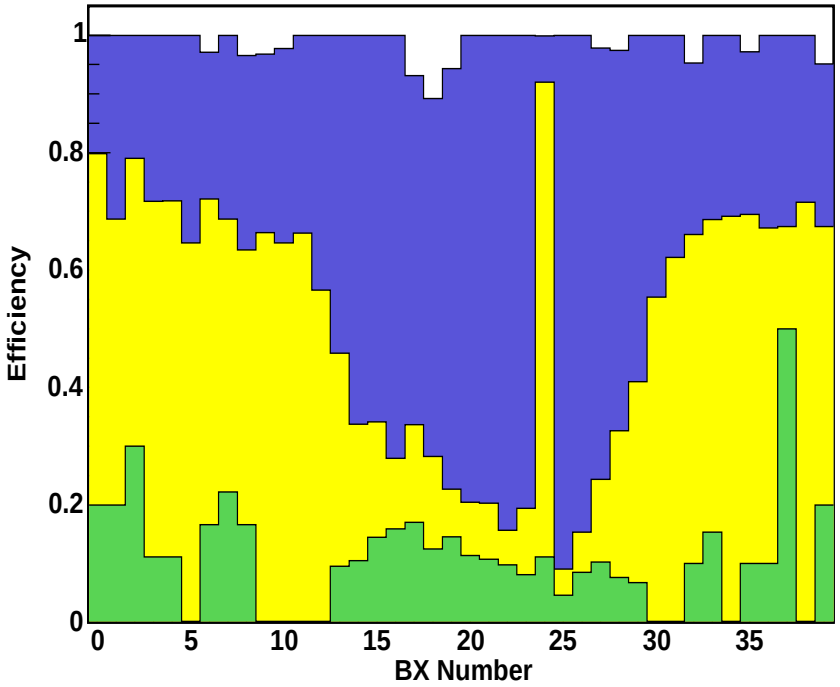

Figure 24: Efficiency to reconstruct a trigger track by the DTTF, as a function of the BX (light grey or yellow histogram). The correct BX is 24. Superimposed are the efficiency to reconstruct a trigger track when there is a coincidence of two trigger segments both of HH quality (dark grey or blue), and a coincidence of two trigger segments both of L quality (medium grey or green).

HH coincidences is 99.7 $\pm$ 0.1 %. This fits with the expectations, as such tracks are real muon tracks crossing the apparatus. On the other hand, when the trigger segments have a low quality, which is typical of fake triggers, the DTTF ghost suppression is very effective. The shape of the dark grey or blue curve reflects the relative amounts of muons and ghosts as a function of the BX. The rejection power for ghosts (L coincidences at BX $\neq$ 24) is 9.5 $\pm$ 0.4. An exception is for BX=24, for which the efficiency is high also for L quality triggers, such events being real muons crossing the apparatus. Therefore, although the out-of-time local trigger rate in a single station is rather high (as shown in figures 13 and 17), it is very unlikely to match such ghost triggers to form a DTTF track.

When a DTTF track is found, it is made by two segments (one in MB1 and one in MB3) which in general have different quality. Figure 25 is a lego plot which shows the correlation between the quality of the local trigger segment in MB1 versus MB3. Only segments at the correct BX are considered. The DTTF matching efficiency is defined as the efficiency for the DTTF system to match two segments from the two muon stations and form a track. When the two segments have both HH quality, the matching efficiency is higher than 99 %. When the quality of the two segments is poorer than HH, the matching efficiency is 86 %. The inclusive matching efficiency, at the correct BX, is 94 %.

6 Conclusions

Two drift tubes muon stations of the CMS muon barrel system were exposed, in October 2004, to a 40 MHz bunched muon beam at the Cern SpS. The performance of the level-1 local trigger was tested at different energies and inclination angles of the incident muon beam. Data with and without an iron absorber placed between the two stations were also collected, to simulate the electromagnetic shower development in CMS. The effect of the absorber is to decrease the BX identification efficiency by about 3 %, when the muon momentum is increased from 50 to 300 GeV/c due to the development of electromagnetic showers. Due to a wrong configuration of the θ BTIs, the comparison with the emulation, which does not reproduce such a problem, is not straightforward. Therefore dedicated runs were emulated by introducing the wrong BTIs configuration in the simulation code, and in these cases the agreement between trigger data and trigger emulator is found to be excellent. Special data-taking runs were dedicated to test the ϕ DTTF trigger for the first time. The system performed in an excellent manner, showing a high efficiency to reconstruct tracks at the correct BX, and a good rejection power to discard ghosts at wrong BXs.

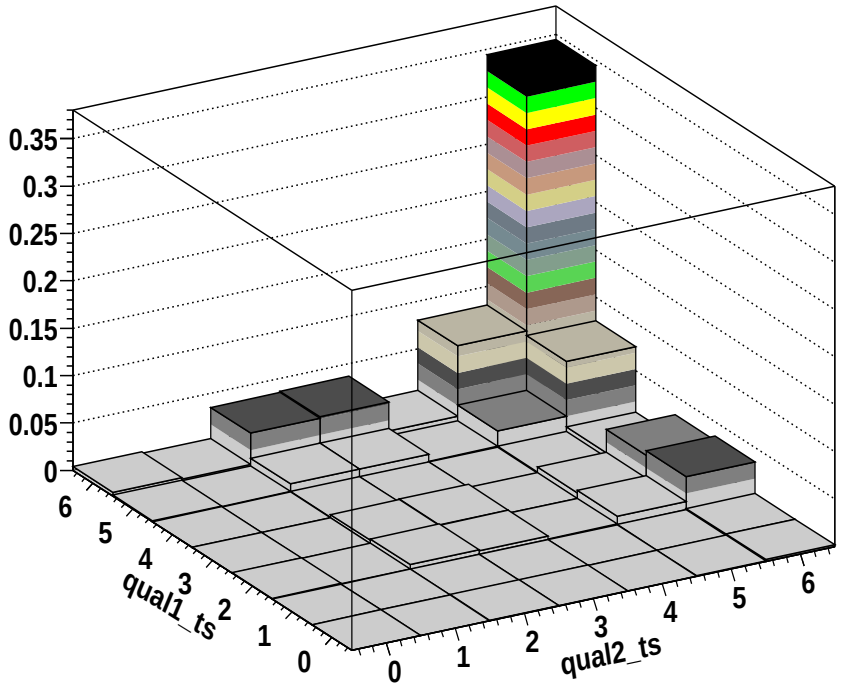

Figure 25: Correlation between the quality of the local trigger segment in MB1 (qual1) versus MB3 (qual2). Only segments at the correct BX are considered. When the two segments have both HH quality, the DTTF matching efficiency (defined in the main text) is 99 %. When the quality of the two segments is poorer than HH, the matching efficiency is 86 %. The inclusive matching efficiency is 94 %.

Acknowledgements

We acknowledge the support of the staff of the electronics and mechanical workshops of INFN Bologna, INFN Padova, RWTH Aachen and CIEMAT. In particular we are grateful to L. Barcellan, M. Boldini, V. Cafaro, G. Fetchenhauer and V. Giordano for their valuable technical help. We acknowledge the help of G. Bencze who provided the scintillator set-up used as an external muon trigger. Furthermore we acknowledge the support by the German "Bundesministerium für Bildung und Forschung" (BMBF) and the Austrian Federal Ministry for Education, Science and Culture. C. Deldicque, J. Erö, I. Jiménez, and J. Fernández de Trocóniz are also grateful for support by the Austrian Exchange Service and the Spanish Ministry of Science through the Acciones Integradas program, under project numbers 21/2004 and HU 2003-0012.

References

[1] CMS, Technical Proposal, CERN/LHCC 94-38, LHCC/P1,1994.

[2] CMS, The Muon Project, Technical Design Report, CERN/LHCC 97-32.

[3] CMS, The Level-1 Trigger, Technical Design Report, CERN/LHCC 2000-038.

[4] P. Arce et al., Nucl. Instrum. and Meth. A 534 (2004), 441-485.

[5] M. Aguilar-Benitez et al., Nucl. Instrum. and Meth. A 480 (2002) 658, and references therein.

[6] B. Taylor, IEEE, Trans. Nuclear Science, Vol. 45 (1998).

[7] G.M. Dallavalle et al., Proceedings of the 4th Workshop on Electronics for LHC Experiments, Rome, Sept 98, page 294.